The Effects of Ar-ion Bombardment and Annealing of D_2O/Zircaloy-4 Surfaces Using XPS and UPS

Kyung-Sun Oh and Yong-Cheol Kang*

*Department of Chemistry, Pukyong National University, Busan 608-737, Korea. *E-mail: yckang@pknu.ac.kr*
Received May 7, 2007

The surface chemistry of D_2O dosed Zircaloy-4 (Zry-4) surface followed by Ar-ion bombardment and annealing was studied by means of X-ray photoelectron spectroscopy (XPS) and Ultraviolet photoelectron spectroscopy (UPS). In the XPS study, Ar-ion bombardment caused decrease of the oxygen on the surface region of Zry-4 and therefore led to change the oxidation states of the zirconium from oxide to metallic form. In addition, oxidation states of zirconium were changed to lower oxidation states of zirconium due to depopulation of oxygen on the surface region by annealing. Up to about 787 K, the bulk oxygen diffused out to the subsurface region and after this temperature, the oxygen on the surface of Zry-4 was depopulated. UPS study showed that the valence band spectrum of the D_2O exposed Zry-4 exhibited a dominant peak at around 13 eV and no clear Fermi edge was detected. After stepwise Ar^+ sputtering processes, the decrease of the oxygen on the surface of Zry-4 led to suppress the dominant peak around 13 eV, the peak around 9 eV and develop a new peak of the metallic Zr 4d state (20.5-21.0 eV) at the Fermi level.

Key Words : Zircaloy-4, D_2O, X-ray photoelectron spectroscopy, UV Photoelectron spectroscopy

Introduction

Zry-4 is widely used in the nuclear industry as cladding materials for fuel containment in nuclear reactors, those are cooled by water/heavy water, because of its corrosion resistive property and low thermal neutron scattering cross-section. The corrosion,[1-4] oxidation[5-8] or hydrogen absorption kinetics[9-12] of Zry-4 and its nuclear applications have been of great concern and investigated with a variety of surface science techniques in the literatures. Zry-4 oxidation by water (H_2O) and steam environments has been reported in numerous studies.[13-18] The interaction of H_2O with Zry-4 was investigated using Auger electron spectroscopy (AES) and Temperature programmed desorption (TPD) methods by R. D. Ramsier *et al.*.[13] They reported that following adsorption of H_2O at 150 K, the Zr(MNV) and Zr(MNN) Auger features shifted by ~6.5 and 4.5 eV, respectively, indicating surface oxidation. Heating H_2O/Zry-4 resulted in molecular desorption of water at both low and high temperatures. The effects of adsorbates on the oxidation of Zry-4 in air and steam were studied by the measurement of the weight gain of specimens.[14] They reported that the effect of LiOH was dependent on the surface condition, temperature and the type of atmosphere. The behavior of water with sulfur dioxide pre-exposed Zry-4 surfaces was also studied in R. D. Ramsier's group.[15] They reported that adsorption of SO_2 caused shift of the Zr(MNN) Auger electron feature by 3.0 eV, whereas subsequent water adsorption attenuated the sulfur Auger signal and resulted in the development of a zirconium oxide, Zr(MNN), feature. However, despite the fact that a number of articles deal with the interaction of D_2O on zirconium,[19,20] little is known about the surface chemistry of deuterium containing species on Zry-4 surfaces.[21,22]

In this work, the effects of Ar-ion bombardment and annealing on the surface of D_2O dosed Zry-4 surface were investigated using XPS and UPS.

Experimental Section

Zry-4 sample in this work has a surface area of 29.22 mm^2 from a sheet of Zry-4. Its elemental composition is nominally 1.2-1.7 wt% Sn, 0.18-0.24 wt% Fe, 0.07-0.13 wt% Cr, 0.08-0.015 wt% O and the balance Zr.[23] The Zry-4 sample was polished with abrasive papers and a mechanical polisher (Buehler, gamma alumina, 0.05 micron). After mechanical treatment, it was ultrasonically degreased in acetone for 20 min after dried with nitrogen gas. After ex situ D_2O (99.999% purity, Aldrich) dosing on Zry-4, the specimen was installed in an ultra high vacuum (UHV) chamber. The UHV chamber used in this study was pumped by two stages of pumping system and the pumping system is the same as the previous paper.[24]

The XPS and UPS experiments were carried out in UHV (base pressure 7.5×10^{-11} torr) chamber equipped with a concentric hemispherical analyzer (CHA), a twin anode X-ray source (Mg and Al Kα 1253.6 and 1486.6 eV, respectively) for XPS (VG ESCALAB 2000) and a UV source (He I 21.2 eV, He II 40.8 eV) for UPS.

During survey scans, XP spectra were obtained using Al Kα x-ray source. X-ray source was at high voltage of 15 kV, beam current of 15 mA, filament current of 4.2 A, pass energy of 20 eV, dwell time of 50 ms and energy step size of 1 eV in constant analyzer energy (CAE) mode at large area XPS (LAXPS) for annealing and small area XPS (SAXPS) for study of Ar-ion bombardment effect and other factors were same as the parameters used in the investigation of annealing effect. He I was used as the exciting source for UPS measurements. Pass energy of 2 eV, energy step size of

0.05 eV and large area UPS mode were applied for UPS survey scan and narrow scan. D_2O dosed Zry-4 sample was pre-pumped in the fast entry air loadlock (FEAL) chamber for approximately 2 hrs before loading into the analysis chamber which was pumped by a turbo molecular pump (TMP, 70 L/s) backed by a roughing pump (RP, 200 L/min). Obtained XPS Zr3d and O1s peaks were divided into several peaks according to their chemical environments by means of deconvolution process. The full width half maximum (FWHM) of each peak of Zr3d and O1s were between 1.3 and 2.5 eV, 1.5 and 2.3 eV, respectively, and G/L ratio of 27% (Lorentzian-27%, Gaussian-73%). Our XPS data were deconvoluted using XPSPEAK software (ver 4.1).

During Ar (99.999% purity, Aldrich) ion bombardment, the argon pressure was kept at 7.5×10^{-8} torr, the sample current was about 2.02 μA and the argon fluence was 0.52×10^{16} Ar^+/cm^2 per 1 cycle of Ar^+ sputtering. In the UPS measurements, the sample current was about 1.65 μA and the argon fluence was 0.39×10^{16} Ar^+/cm^2 per 1 cycle of Ar^+ sputtering.

Results and Discussion

Figure 1 presents the Zr3d (a) and O1s (b) XP spectra of D_2O exposed Zry-4 sample after different Ar^+ fluences (indicated in each spectrum). Prior to Ar^+ sputtering (bottom line in Figure 1(a)), the XP spectra of Zr3d showed four elementary peaks of different Zr3d states. The intensities of high binding energy peaks of $Zr3d_{5/2}$ around 183.7 eV and 182.8 eV were reduced those were assigned for ZrO_2 and ZrO_x ($1 < x < 2$), respectively. Whereas the peaks at low binding energy around 179.4 eV and 181 eV were gradually dominated as the Ar^+ fluence was increasing in the amounts. Those peaks were assigned for metallic zirconium and ZrO_x ($0 < x < 1$).[25,26] The values of the peaks were in good agreement with previous work.[27] In Figure 1(b), the O1s spectra were composed by two components centered at about 532.9 and 531.1 eV which were attributed to OD and O^{2-}, respectively.[6,27-29] The peak around 532.9 eV was

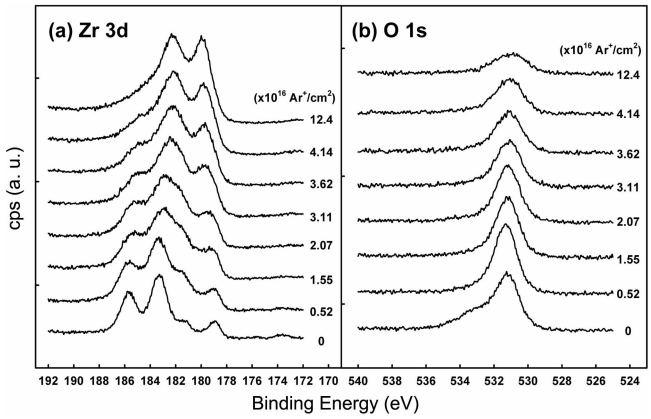

Figure 1. XP spectra of the Zr3d (a) and O1s (b) of D_2O exposed to Zircaloy-4 surfaces after different Ar^+ fluences.

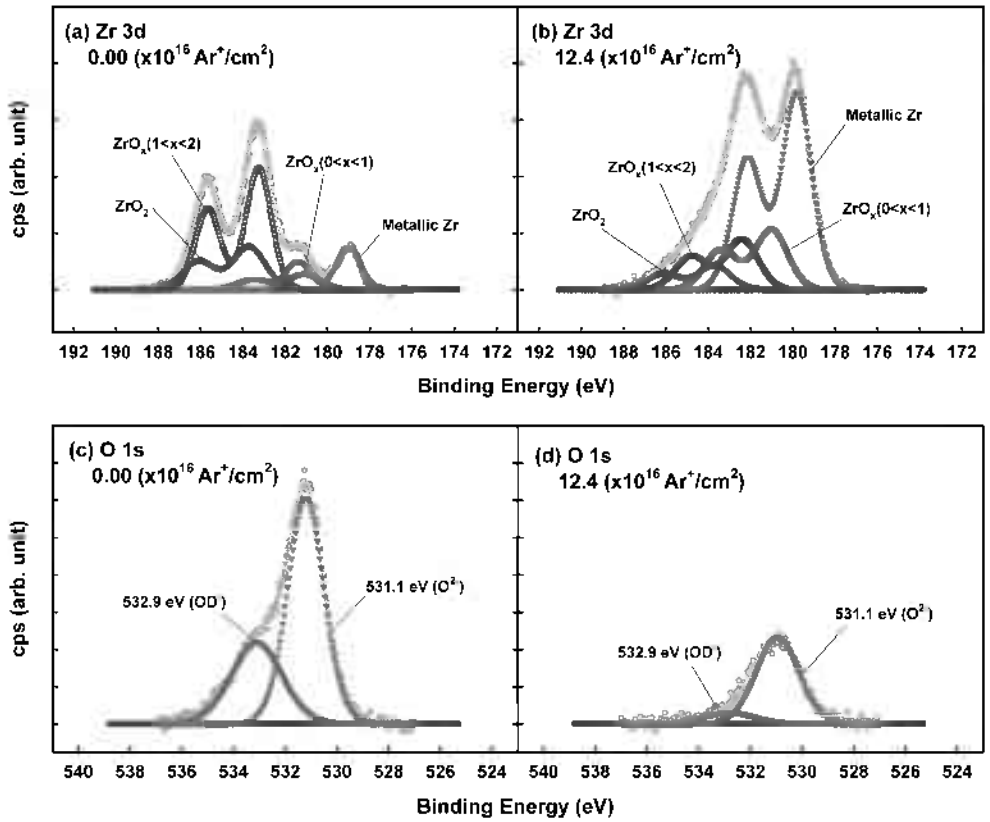

Figure 2. Deconvolution of measured Zr3d and O1s spectra of the D_2O exposed to Zircaloy-4 after different Ar^+ fluences (a) Zr3d: 0.00×10^{16} Ar^+/cm^2 (b) Zr3d: 12.4×10^{16} Ar^+/cm^2. (c) O1s: 0.00×10^{16} Ar^+/cm^2 (d) O1s: 12.4×10^{16} Ar^+/cm^2.

almost disappeared and the peak at 531.1 eV was increased at the initial stage of Ar-ion bombardment then decreased after further Ar-ion bombardment.

The peak deconvolution of Zr3d and O1s spectra of D_2O exposed Zry-4 before and after Ar^+ sputtering (Ar^+ fluence; 12.4×10^{16} Ar^+/cm^2) are depicted in Figure 2(a)-(d). The Zr3d peaks (spin orbit splitting is 2.4 eV) at 183.7, 182.8, 181 and 179.4 eV were attributed to ZrO_2, ZrO_x ($1 < x < 2$), ZrO_x ($0 < x < 1$) and metallic zirconium, respectively.[5,25,26] The oxygen as OD^- form was almost removed and the oxygen of O^{2-} form was considerably reduced after Ar^+ bombardment. The effect of the Ar^+ bombardment was clearly observed as shown in Figure 1 and 2. Ar^+ bombardment caused a decrease of oxygen on the surface of Zry-4 and therefore led to change the oxidation state of the zirconium from ZrO_2 to metallic zirconium.

The peak intensities of the different oxidation states of zirconium as a function of the Ar^+ fluence have been depicted in Figure 3. At the initial stage of Ar^+ bombardment, the O1s intensity of surface oxygen form was increased then gradually decreased with further Ar^+ bombardment (Figure 3(a)). This phenomenon caused sudden increase of ZrO_x ($0 < x < 2$) then decrease as shown in Figure 3(a). Up

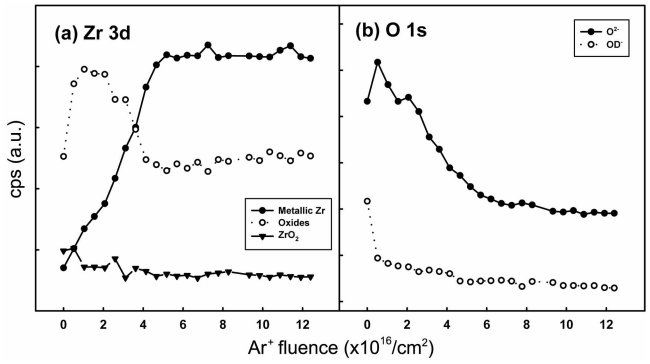

Figure 3. The relative ratios of the Zr3d (a) and O1s (b) peaks of the surface of D_2O exposed to Zircaloy-4 as a function of the Ar^+ fluence.

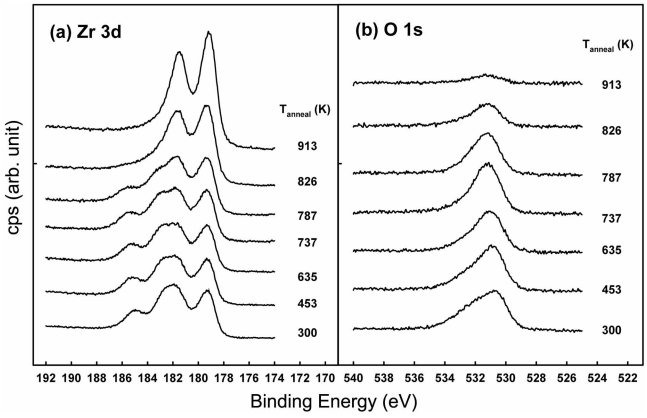

Figure 4. XP spectra of the Zr3d (a) and O1s (b) of D_2O exposed to Zircaloy-4 after stepwise annealing process.

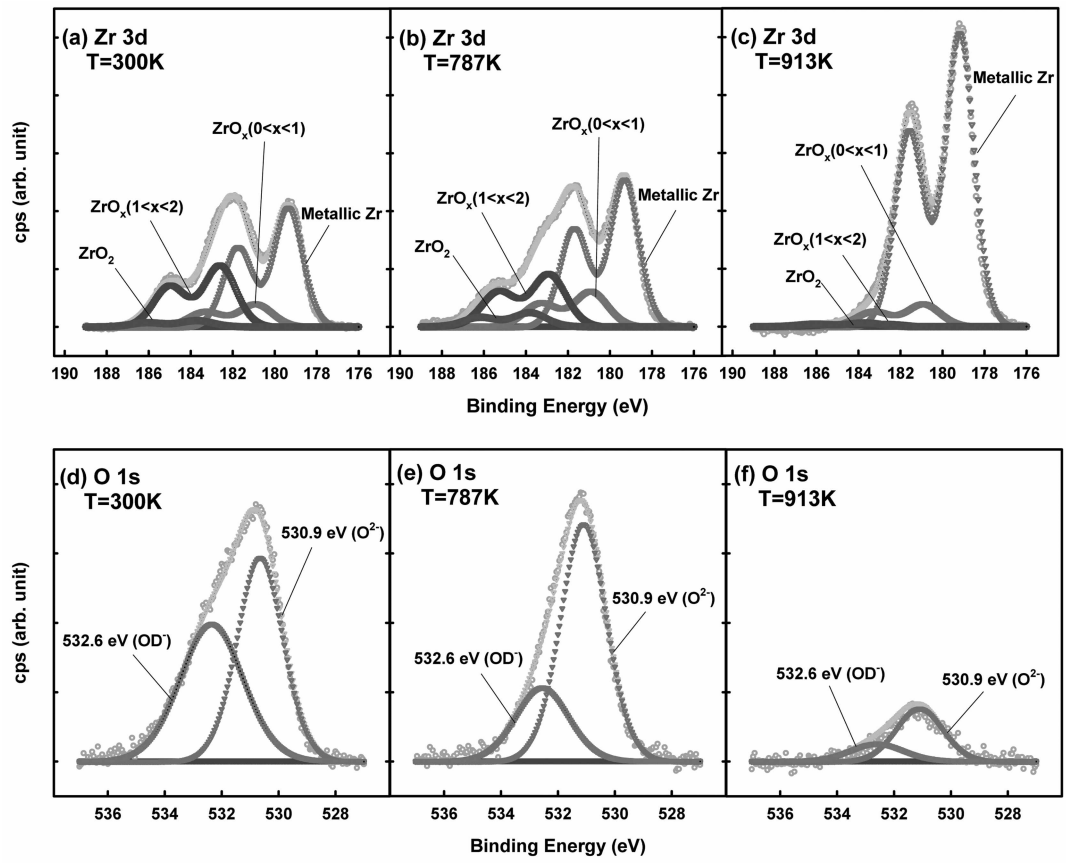

Figure 5. Deconvolution of measured Zr3d and O1s spectra of D_2O exposed to Zircaloy-4 after thermal treatment (a) Zr3d: 300 K (b) Zr3d: 787 K (c) Zr3d: 913 K, (d) O1s: 300 K (e) O1s: 787 K (f) O1s: 913 K.

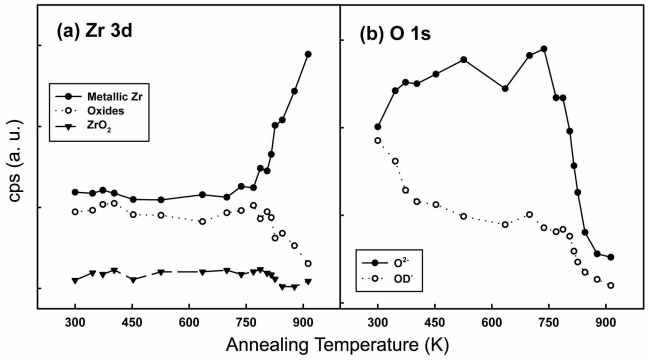

Figure 6. The relative ratios of the Zr3d (a) and O1s (b) peaks of the surface of D_2O exposed to Zircaloy-4 as a function of annealing temperature.

to around 5×10^{16} Ar^+/cm^2, surface oxygen was depopulated at a certain level then the ratios of the peaks were stayed constant level. This study showed that Ar^+ bombardment was limited to recover metallic zirconium from D_2O dosed Zry-4.

Figure 4(a) and (b) represent the evolution of the XP spectra in the Zr3d and O1s region of D_2O dosed Zry-4 after stepwise thermal treatment. The Zr3d and O1s XP spectra were composed of several peaks which were assigned ZrO_2 (183.7 eV), ZrO_x ($1 < x < 2$, 182.6 eV), ZrO_x ($0 < x < 1$, 180.9 eV) and metallic zirconium (179.3 eV) as shown in Figure 2 and 5. Zr3d XP spectra are stacked up by the annealing temperature in Figure 4(a). Decrease of the Zr3d peak intensities at 183.7 and 182.6 eV, which was intense at room temperature, was observed with increasing the annealing temperature and almost vanished at 913 K. While the peak around 179.3 eV was increased at higher temperature and dominated at 913 K. In Figure 4(b), the peak shape was changed by annealing temperature. At the highest temperature, the O1s peak was almost disappeared. We analyzed the peak shape change by deconvolution process.

The deconvoluted peaks at the different annealing temperatures are shown in Figure 5. Up to 787 K, the O1s peak of O^{2-} around 530.9 eV was dominated because the bulk oxygen diffused out to the subsurface region. After that, surface oxygen was depopulated as D_2O desorption. After 787 K, the O1s intensity was decreased dramatically. This caused the decrease of all of the zirconium oxide species (ZrO_2, ZrO_x ($0 < x < 1$ and $1 < x < 2$)) and increase of metallic zirconium.

Figure 6 shows the integrated areas of detailed Zr3d and O1s in different chemical environments by the annealing temperature. Annealing of D_2O dosed Zry-4 surface results in depopulation of oxygen at the surface. This caused conversion of zirconium oxides (ZrO_x, $0 < x < 2$) to metallic zirconium.

Due to the lower kinetic energy of the electrons excited from the valence band, UPS has a higher surface sensitivity than XPS.[30] The changes of the valence band structures of D_2O exposed Zry-4 after stepwise Ar-ion sputtering processes were studied by means of UPS. The UP spectra were

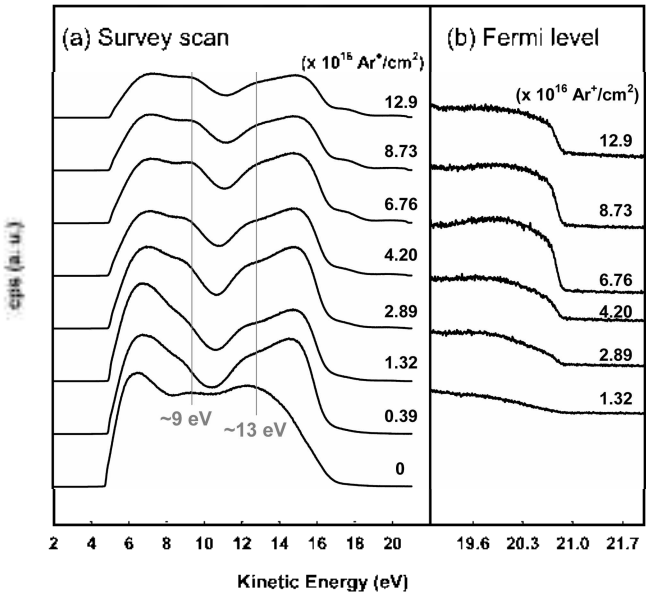

Figure 7. UP spectra of D_2O exposed Zircaloy-4 after Ar-ion sputtering (a) survey scan and (b) high resolution UP spectra near Fermi level.

obtained by using He I as the exiting source, those are shown in Figure 7. The substrate valence band was dominated mainly by the O2p and Zr4d orbitals extending from approximately 5 to 16 eV of kinetic energy as shown in Figure 7(a). The window of valence band spectra observed in this study is little bit wider than the result of valence band experiment by Sanz *et al.*.[31] The valence spectrum of the D_2O exposed Zry-4 exhibited a dominant peak at around 13 eV which could be assigned to surface ZrO_2 and was attributed to emission from O2p states interacting with the d-bands of zirconium (bottom line in Figure 7(a)).[30,32] The shoulder centered at about 9 eV could be correlated with surface OH which is commonly present on untreated metal surfaces.[30] No Fermi edge was observed in the initial state of Ar^+ sputtering as shown in Figure 7(a). After stepwise Ar^+ sputtering process, however, there were significant changes of the valence band spectrum, such as the dominant peak around 13 eV and the shoulder peak about 9 eV were decreased and the Fermi edge was emerged as shown in Figure 7(b). The decrease of the oxygen on the surface of Zry-4 by Ar^+ sputtering led to suppress the dominant peak (ZrO_2, ~13 eV), the peak around 9 eV as surface hydroxide, and develop a new peak of the metallic Zr4d state (20.5-21.0 eV) at the Fermi level.

Conclusions

The surface chemistry of D_2O exposed Zry-4 system was investigated about Ar-ion bombardment and annealing effects using XPS and UPS. In XPS study, the effects of the Ar^+ bombardment and annealing were clearly observed. The gradual depletion of oxygen on the surface region was occurred upto 5.0×10^{16} of Ar fluence. After this Ar fluence, the amount of oxygen on the surface region was stayed at a

certain constant level. The decrease of oxygen on the surface region caused the change of oxidation states of zirconium from zirconium oxides to metallic zirconium. This implies that Ar^+ bombardment was limited to regain the metallic zirconium from zirconium oxides (ZrO_x, $0 < x < 2$). Annealing of the D_2O dosed Zry-4 system also caused removal of the oxygen on the surface region. After 787 K, the oxygen peak was dramatically decreased and almost pure metallic zirconium was obtained at 913 K. UPS study showed the dominant peak around 13 eV (emission from O2p state). the peak around 9 eV (surface hydroxide peak) decreased and the new peak of the metallic Zr4d state at the Fermi level (20.5-21.0 eV) developed as the oxygen vanished after stepwise Ar^- sputtering. This result supports well the XPS data.

Acknowledgement. This work was supported by the Brain Korea 21 Project Second Phase in 2006. And special thanks to Young-Cheol Ryu at Cooperative Laboratory Center in PKNU.

References

1. Wan, Q.; Bai, X.; Zhang, X. *Mater. Res. Bull.* **2006**, *41*, 387.
2. Kim, W.; Jung, K. S.; Choi, B. H.; Kwon, H. S.; Lee, S. J.; Han, J. G.; Guseva, M. I.; Atamanov, M. V. *Surf. Coat. Technol.* **1995**, *76*, 595.
3. Chen, X. W.; Bai, X. D.; Deng, P. Y.; Peng, D. Q.; Chen, B. S. *Nucl. Instr. and Meth. B* **2003**, *211*, 512.
4. Liu, X.; Bai, X.; Zhou, C.; Wei, L. *Surf. Coat. Technol.* **2004**, *182*, 138.
5. Bai, X. D.; Wang, S. G.; Xu, J.; Bao, J.; Chen, H. M.; Fan, Y. D. *J. Nucl. Mater.* **1998**, *254*, 266.
6. Li, J.; Bai, X.; Zhang, D.; Li, H. *Appl. Surf. Sci.* **2006**, *252*, 7436.
7. Stojilovic, N.; Ramsier, R. D. *J. Nucl. Mater.* **2006**, *350*, 163.
8. Berger, P.; El Tahhann, R.; Moulin, G.; Viennot, M. *Nucl. Instr. and Meth. B* **2003**, *210*, 519.
9. Meyer, G.; Kobrinsky, M.; Abriata, J. P.; Boleich, J. C. *J. Nucl. Mater.* **1996**, *229*, 48.
10. Gümez, M. P.; Domizzi, G.; Lüpez Pumarega, M. I.; Ruzzante, J. E. *J. Nucl. Mater.* **2006**, *353*, 167.
11. Kim, S. J.; Kim, K. H.; Baek, J. H.; Choi, B. K.; Jeong, Y. H.; Jung, Y. H. *J. Nucl. Mater.* **1998**, *256*, 114.
12. Fernández, G. E.; Meyer, G.; Peretti, H. A. *J. Alloys & Compd.* **2002**, *330*, 483.
13. Stojilovic, N.; Ramsier, R. D. *Appl. Surf. Sci.* **2006**, *252*, 5839.
14. Park, K. H.; Cho, Y. C.; Kim, Y. G. *J. Nucl. Mater.* **1999**, *270*, 154.
15. Stojilovic, N.; Ramsier, R. D. *Surf. Interface Anal.* **2006**, *38*, 139.
16. Hong, H. S.; Moon, J. S.; Kim, S. J.; Lee, K. S. *J. Nucl. Mater.* **2001**, *297*, 113.
17. Bai, X.; Xu, J.; He, F.; Fan, Y. *Nucl. Instr. and Meth. B* **2000**, *160*, 49.
18. Stojilovic, N.; Bender, E. T.; Ramsier, R. D. *J. Nucl. Mater.* **2006**, *348*, 79.
19. Li, B.; Griffiths, K.; Zhang, C.-S.; Norton, P. R. *Surf. Sci.* **1997**, *370*, 97.
20. Kang, Y. C.; Ramsier, R. D. *Surf. Sci.* **2002**, *519*, 229.
21. Takagi, I.; Hashizumi, M.; Yamagami, A.; Maehara, K.; Higashi, K. *J. Nucl. Mater.* **1997**, *248*, 306.
22. Gobrecht, K.; Gutsmiedl, E.; Scheuer, A. *Phy. B* **2002**, *311*, 148.
23. Charquet, D.; Hahn, R.; Ortlieb, E.; Gros, J. P.; Wadier, J. F. *Zirconium in the Nuclear Industry*; San Diego, 1989; STP 1023, p 405.
24. Kwon, J. H.; Youn, S. W.; Kang, Y. C. *Bull. Korean Chem. Soc.* **2006**, *27*, 11.
25. Lyapin, A.; Jeurgens, L. P. H.; Mittemeijer, E. J. *Acta Mater.* **2005**, *53*, 2925.
26. Lyapin, A.; Jeurgens, L. P. H.; Graat, P. C. J.; Mittemeijer, E. J. *J. Appl. Phys.* **2004**, *96*, 12.
27. Roustila, A.; Chêne, J.; Séverac, C. *J. Alloys & Compd.* **2003**, *356*, 330.
28. Morant, C.; Sanz, J. M.; Galán, L. *Phys. Rev. B* **1992**, *45*, 3.
29. Wiame, H.; Centeno, M. A.; Picard, S.; Bastians, P.; Grange, P. *J. Eur. Ceram. Soc.* **1998**, *18*, 1293.
30. Song, Z.; Bao, X.; Wild, U.; Muhler, M.; Ertl, G. *Appl. Surf. Sci.* **1998**, *134*, 31.
31. Sanz, J. M.; Gonzalez-Elipe, A. R.; Fernandez, A.; Leinen, D.; Galan, L.; Stampfl, A.; Bradshaw, A. M. *Surf. Sci.* **1994**, *307*, 848.
32. Zafeiratos, S.; Neophytides, S.; Kennou, S. *Thin Solid Films* **2001**, *386*, 53.